Nuclear Materials and Energy 40 (2024) 101689

Contents lists available at ScienceDirect

Nuclear Materials and Energy

journal homepage: www.elsevier.com/locate/nme

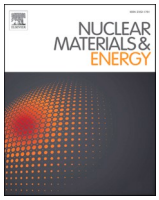

Thermal hydraulic and structural analysis of the IFMIF-DONES liquid-lithium target system

S. Gordeev [a,*], A. Serikov [a], Y. Qiu [a], F.S. Nitti [b], J. Maestre [c]

[a] Karlsruhe Institute of Technology, Eggenstein-Leopoldshafen, Germany
[b] ENEA Brasimone, Italy
[c] University of Granada, Spain

ARTICLE INFO

Keywords:
IFMIF-DONES
Lithium Target
CFD
FEM
Thermal-hydraulics
Thermal-Mechanics

ABSTRACT

In the IFMIF-DONES neutron source a single accelerator line delivers 125 mA of deuterons at 40 MeV to a flowing liquid lithium target with a free surface facing the deuteron beam.

Neutrons with fusion-relevant spectrum are generated by a stripping reaction and used for material samples irradiation.

This report presents a numerical thermal–hydraulic and structural analysis using updated design of the target system and neutronics analysis results. Simulation scope includes the target assembly, vacuum chamber with beam ducts, outlet channel, quench tank vessel and connecting elements.

Simulations have been conducted with the commercial CFD code Simcenter Star-CCM + . The computational domains consist total of $47.4x10^6$ fluid and $14x10^6$ structure cells.

The following aspects have been analyzed:

- Temperature distribution in lithium and target system structure during beam-on operation;
- Transient mixing of lithium in the quench tank with temperature change during the beam switch-on phase.
- Thermal displacements and stresses in the TA and QT structures.

Simulations using the new distribution of nuclear heating show no significant changes in the temperature field in liquid lithium. Calculated unwanted temperature hotspots in the target structure demonstrate the need for optimization of the target design.

Introduction

In the IFMIF-DONES neutron source a single accelerator line delivers 125 mA of deuterons at 40 MeV to a flowing liquid lithium target with a free surface facing the deuteron beam. Neutrons with fusion-relevant spectrum are generated by a stripping reaction and used for material samples irradiation. An up-to-date and well-detailed overview of the IFMIF-DONES facility und the differences between IFMIF and IFMIF-DONES projects can be found in [1].

The high-speed (up to 15 m/s) lithium jet has to maintain a prescribed thickness and to remove the heat providing the desired neutron flux. Hence its operational performance determines the design of the target assembly (TA), and all up-/downstream interfaces such as nozzle, liquid lithium channel and quench tank (QT). The nozzle has to form a stable lithium jet and the quench tank has the function to collect the lithium-flow emerging from the target and deliver it to the lithium piping system under controlled conditions.

The present analysis combines the modelling of the heated lithium flow with the target structure in order to provide the thermal–hydraulic simulations with the conjugate heat transfer. Additionally, the thermal-structural analysis is conducted. Simulation area includes the target assembly, vacuum chamber with beam ducts, outlet channel, quench tank vessel and connecting elements. Simulations have been performed based on CAD/CATIA geometry [2].

* Corresponding author.
E-mail address: sergej.gordeev@kit.edu (S. Gordeev).

https://doi.org/10.1016/j.nme.2024.101689
Received 28 November 2023; Received in revised form 4 June 2024; Accepted 10 June 2024
Available online 14 June 2024

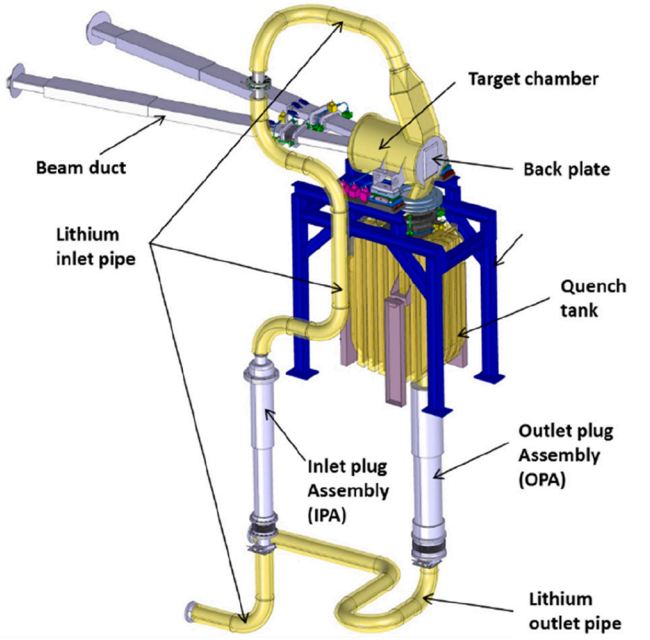

Fig. 1. Current CAD geometry of the Lithium Target and Quench tank.

Calculated energy deposition in the IFMIF-DONES lithium target caused by the transport of four particles: deuteron, neutron, photon, and proton has been calculated adopting the code MCNP6.2 [3]. The dominant contribution to heating in lithium is caused by the interaction of deuteron ions with electrons and nuclei of lithium. The nuclear interactions of deuterons produced secondary particles of neutrons, photons, and protons. The contribution of secondary particles to energy deposition is much less, at the level of a few percent [3]. In the MCNP6.2 neutronics calculations, the radiation source has been defined as a two-dimensional horizontal-vertical matrix based on so-called "IFMIF/EVEDA profile". The difference with the previous source definition is in the approach used: instead of the analytic profile [4], the profile was defined as a 2D matrix [3]. Using the matrix approach of D + beam definition in MCNP, the beam profile could be updated from the High Energy Beam Transport (HEBT) accelerator data. Following the new matrix approach of deuteron beam definition calculations using the IFMIF/EVEDA beam profile has been applied for MCNP6.2 energy deposition.

The aim of this work is to estimate the changes in temperature fields in the lithium flow and target structure caused by the new nuclear heating data. The information obtained, together with the determined thermal stresses and deformations in the entire structures, forms a good basis for further detailed analyses of the flow behavior and optimization of TA design.

CFD/FEM models based on the current CAD geometry

Fig. 1 shows the current design [5] of main lithium system components.

Following components are used in simulations: lithium inlet pipe, nozzle, beam duct parts, vacuum chamber with supports, back plate with outlet channel and quench tank with supports.

Thermal-hydraulic analysis

Computational domains and boundary conditions

CFD Simulations have been performed using commercial CFD code Simcenter Star-CCM+ [6].

Regardless of the symmetrical structure of the target system, the mesh in the simulation includes the complete geometry without symmetrical conditions. In IFMIF-DONES the alignment of the beam axis to the normal axis of the target impact surface is 9°. It is foreseen for a future upgrade of the facility with a second accelerator as in IFMIF [7]. This situation will cause the asymmetrical distribution of the nuclear heating and thus also the asymmetrical temperature distribution in lithium and in the target structure.

The flow conditions in the examined area are different, especially during the start phase of the "beam-on". The accelerated high-speed lithium flow (up to 15 m/s) in the nozzle and in the irradiated area including the outlet is stable. Thus, the temperature distribution in the lithium flow reaches a steady state within a few seconds. In contrast, the mixed flow in the quench tank is slowed down to 5 m/s or less and is characterised by large vortices [8]. A more or less stable state of the temperature field in the QT can be expected after 30 to 40 s.

Due to the different flow conditions, the calculation area is divided into two computational domains: TA and QT. For each flow area, the calculation time and time step are set individually. The outlet duct was

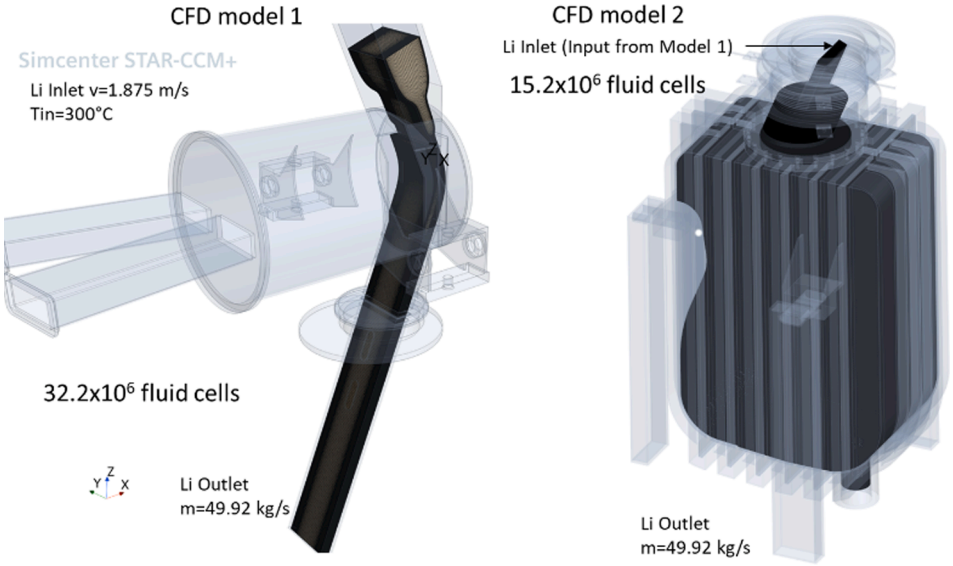

Fig. 2. CFD computational domains for numerical Analysis of Li target and QT.

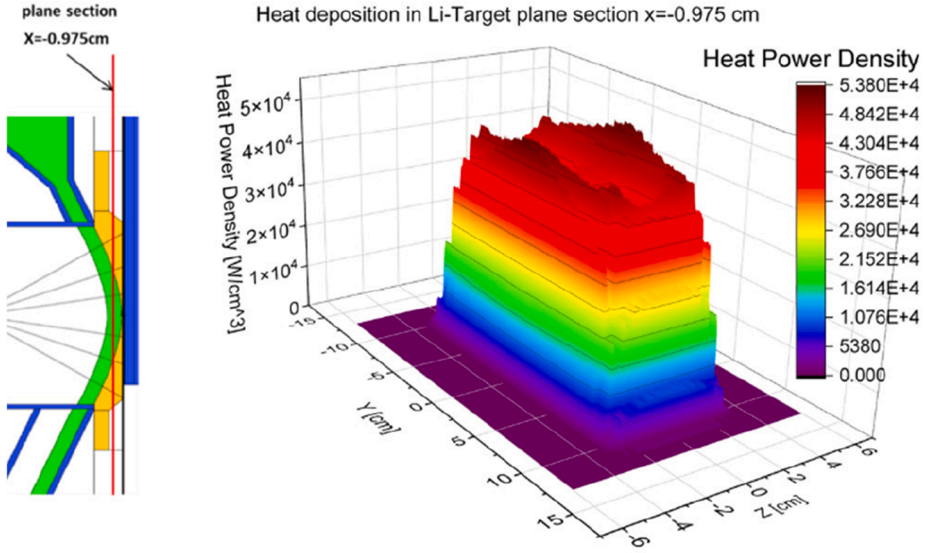

Fig. 3. Nuclear heating of lithium implemented in the model from neutronics [ ] simulations in the cross section x = 0.975 cm.

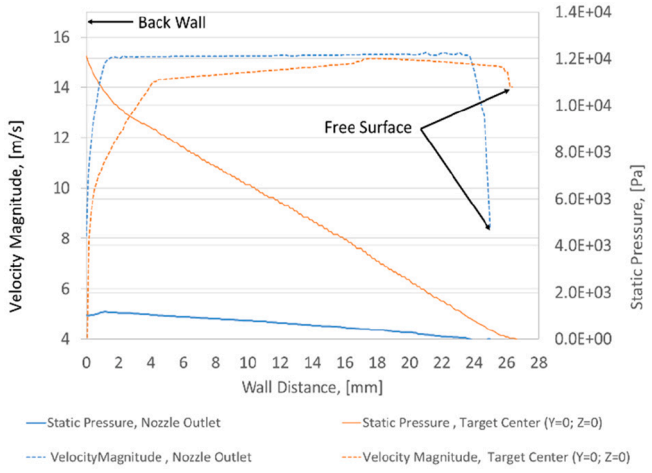

Fig. 4. Static pressure and velocity profiles: at the nozzle outlet (Y = 0) and at the center of the D + beam (Y = 0, Z = 0).

divided into two parts accordingly. The flow parameters from the target outlet in the division cross-section are used as input for the QT area. CFD-computational domains are seen in Fig. 2.

The mesh of the Target model consists of $32.2x10^6$ hexahedral cells with 15 layers in the near wall area. The computational domain of the QT is consisting of the unstructured cell grid with $15.2x10^6$ trimmed cells. Near wall area is meshed by 5 prismatic cells created by cell extrusion. Unstructured meshes offer better flexibility for geometrically complex applications and they are much less sensitive to stretching. Another argument for the unstructured grid is: if the resulting vortices ithin a complex geometry affect the flow behaviour, the alignment of the cell to the streamlines will hardly be possible.

Because of different flow conditions in the near-wall regions the turbulence was modelled by the k-ω Shear-Stress-Transport (SST) model. The turbulence model was applied with automatic wall (All y^+) treatment which allows for a smooth shift from a low-Re number form to a wall function formulation based on the near wall mesh spacing. This model allows the automatic switch of TL/HR treatment depending on the y + value near the wall. Additionally, the model contains a new transport equation for the turbulent dissipation rate, which lets the model satisfy certain mathematical constraints on the normal stresses consistent with the physics of turbulence. The free-surface flow was modelled by means of Volume of Fluid (VOF) method.

In the Target model the cross section 25x260 mm^2 of the nozzle is defined as inlet with constant flow velocity of 1.875 m/s, which corresponds to the target flow velocity of 15 m/s. The lithium Inlet temperature is set to 300 °C. A part of the vacuum chamber backwards to the beam is modelled as pressure outlet boundary. A part of the outlet pipe of the QT is modelled with outlet mass flow rate of 49.92 kg/s.

Fig. 3 illustrates the nuclear heating of lithium implemented in the model from neutronics [3] simulations in the cross section x = 0.975 cm.

Neutronic calculations assume a constant target thickness of 25 mm. In reality, the thickness (or stability) of the lithium beam is influenced by different factors. Some of these, such as turbulent instabilities or Görtler vortices in the nozzle and on the concave wall of the backplate, are not able to change the stability of the free surface of the flow in the long term. One of the effects that noticeably influence the shape of the flowing target in the long term is the centrifugal force caused by the flow along the concave wall. Hydraulic simulations show that the centrifugal acceleration causes the deceleration of the lithium jet and thus the thickening of the target in the irradiation field from 25 mm to 26.5 mm (show Fig. 4). For this reason, the field of the nuclear heating was shifted by 1.5 mm against the beam direction. This corrects the penetration position of the D + beam in the lithium target. The shifted nuclear heating field within the irradiation area is shown in Fig. 5.

Simulation results.

Transient thermal–hydraulic simulations for the beam-on start were conducted for the lithium inlet temperature of 300 °C. Fig. 6 show the temperature field of lithium in TA and QT. The lithium temperature field reaches its steady state in about 30 s. After 30 s, the warm and cold amounts of lithium in the QT are well mixed and the lithium temperature at the outlet reaches the saturation value of 318° C. As shown in Fig. 7 the lithium temperature at the QT outlet is nearly constant with

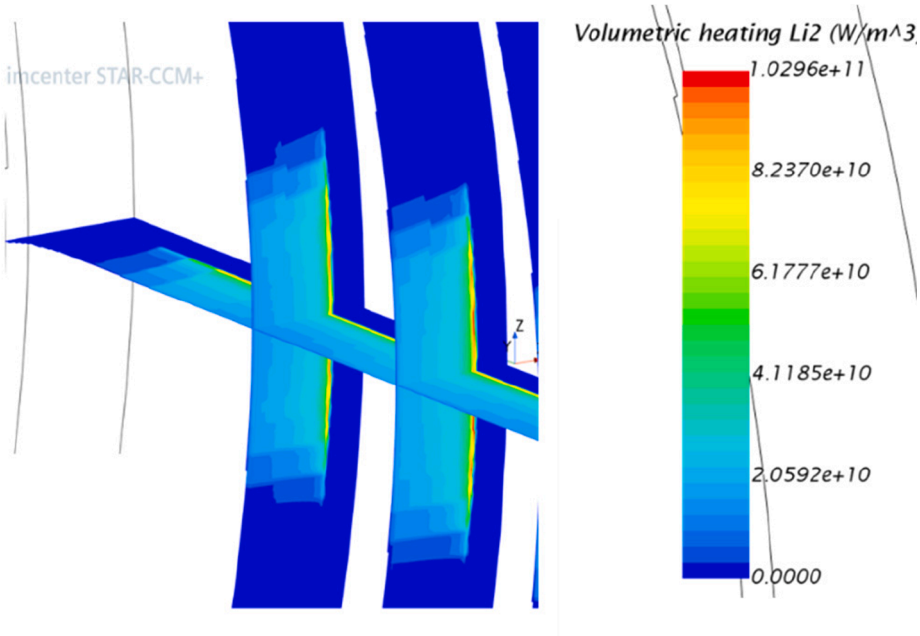

Fig. 5. Nuclear heating with the corrected penetration position of D + beam in lithium target.

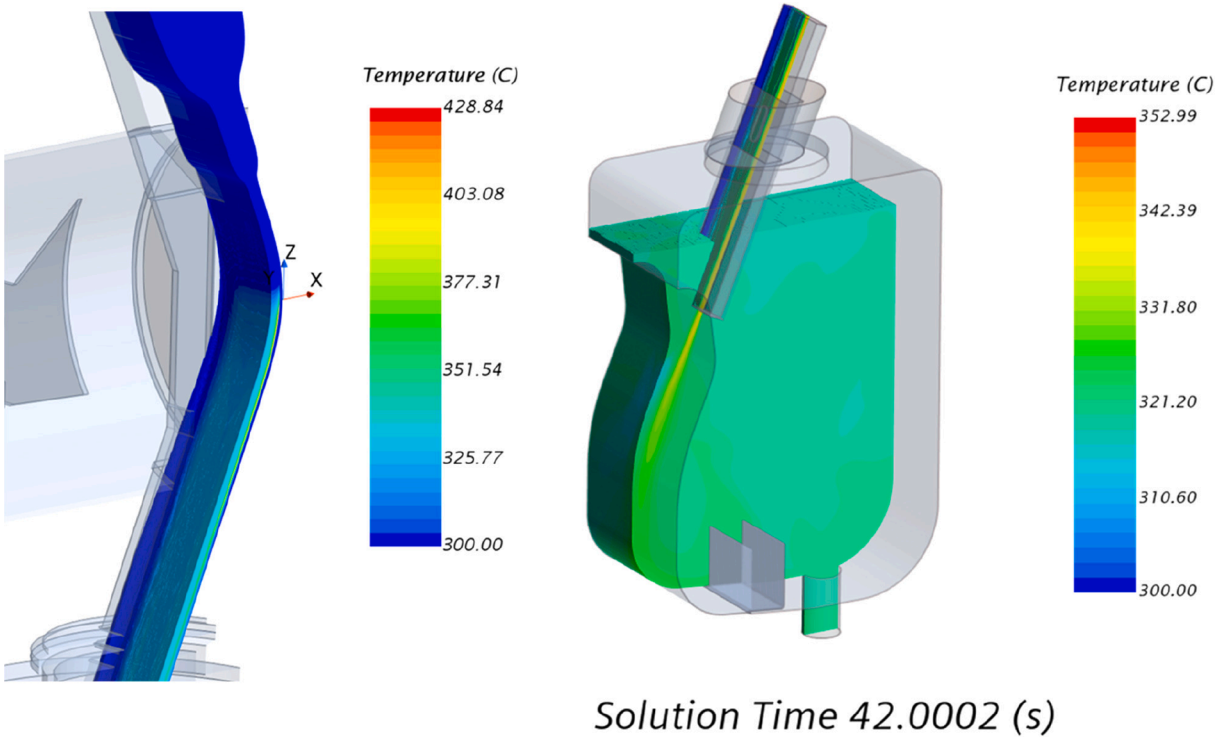

Fig. 6. Temperature distribution in lithium jet and in quench tank.

the maximum difference less than 1 K.

Thermal-structural analysis

The steady state thermal-structural simulations have been conducted using the temperature and heat flux distribution on the contact walls between lithium and structure obtained from the transient thermal–hydraulic simulation for the time step t = 110 s. The analysis was performed with the solid stress model of Simcenter STAR-CCM + using FEM discretization method.

EUROFER 97 was used as the construction material for the TA and the vacuum chamber, and AISI 316L steel for all other components.

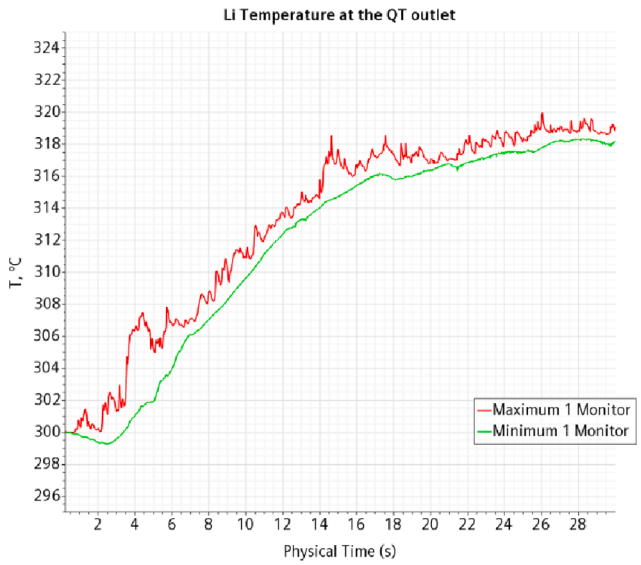

Fig. 7. Maximum and minimum lithium temperature at the QT outlet.

Their temperature-dependent thermophysical properties were taken from [9] and [10].

Computational domain, thermal boundary conditions and mechanical constrains

As shown in Fig. 8a the FEM model consists of the TA including the lithium inlet pipe, vacuum chamber, its support structure, the beam ducts and QT with supports. The flexible connection between TA and QT is ensured by the bellows. The structure was meshed with $13.6x10^6$ tetrahedral cells. The distribution of nuclear heat power deposited within the structural materials has been mapped from [3]. Details of the volumetric heating are depicted in Fig. 8 b, c. Volumetric heating in the isolation material is also taken into account. Fig. 9 shows heat transfer boundary conditions used in simulations. The thermal interaction between outer surfaces and test cell (TC) atmosphere is defined as a heat transfer with the ambient TC temperature of 50 °C and heat transfer coefficient htc = 5 W/m^2 K. Thermal interactions occurring between the TA arms, as well as QT slides and the support structures has been modelled by means of thermal contact models with a thermal conductance of 10 W/m2 K. A radiative and convective heat transfer condition has been imposed to all un-insulated outer surfaces of the model. The heat transfer between the back plate and high flux test module (HFTM) is modelled with the ambient temperature of 150 °C and htc = 1 W/m2 K.

Fig. 10 presents the mechanical constraints for calculation of thermal displacements and stresses. Normal displacement constrains of TA and QT supports allows a free thermal expansion of both structures in the horizontal plane. In order to reduce bending of the supporting legs caused by thermal expansion of the QT a horizontal sliding of three QT connections between the QT and its-supports is allowed. A spatial distribution of the static pressure of lithium on the target surfaces was taken from CFD simulations. Vacuum conditions have been simulated by pressure load of 0.1 MPa applied on the outer surfaces of the TA and QT.

Simulation results

Fig. 11 shows the temperature field in the TA, QT and support structures. Results obtained from the thermal analysis have shown that the maximum temperature within the structure does not exceed the maximum EUROFER allowable temperature of 550 °C. The maximum temperature of 389 °C is predicted to be reached within the vacuum chamber and target structure. The temperature field is slightly asymmetrically distributed, which is due to the beam inclination of 9°.

The total displacement field within the computational domain structure is reported in Fig. 12. The target outlet channel has a maximum expansion of approx. 7 mm inside the quench tank. This could impact the inlet conditions and thus the stable behavior of the liquid lithium in the quench tank. Subsequent simulations with the activation of the fluid–structure interaction models can help to optimize the lithium inlet conditions.

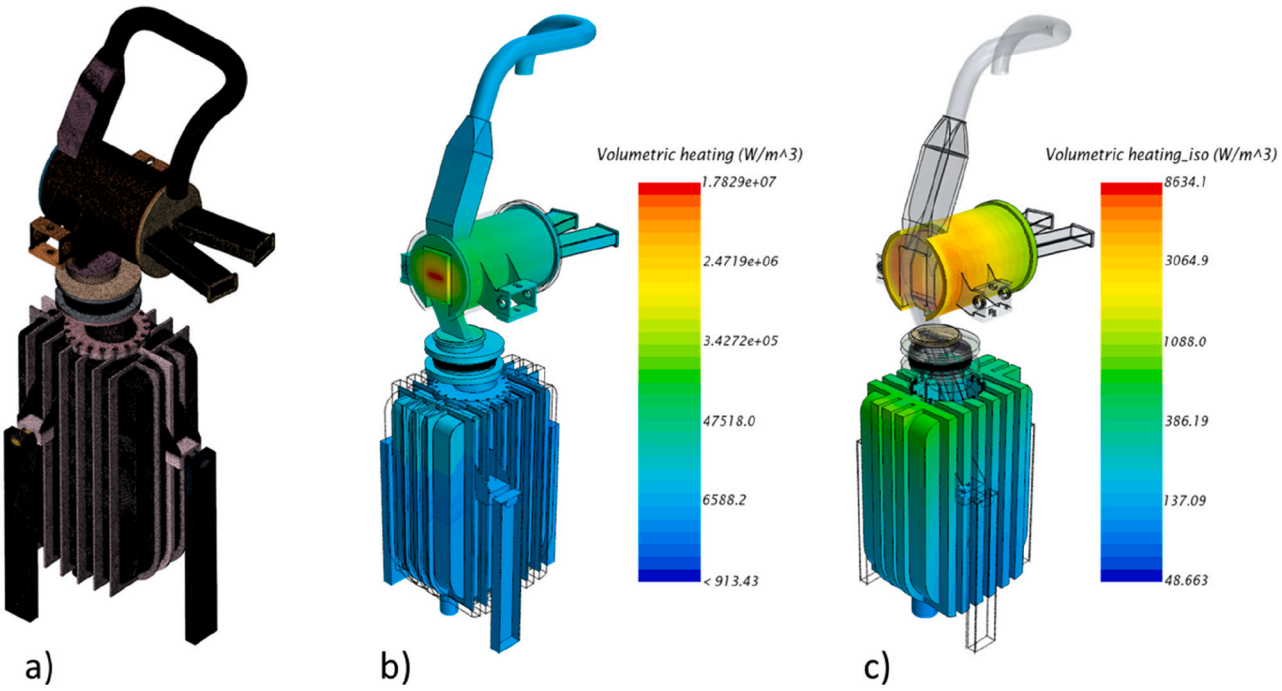

Fig. 8. FEM computational domain for thermal-structural analysis (a), volumetric heating distribution in the TA and QT structure (b), volumetric heating in the insulation (c).

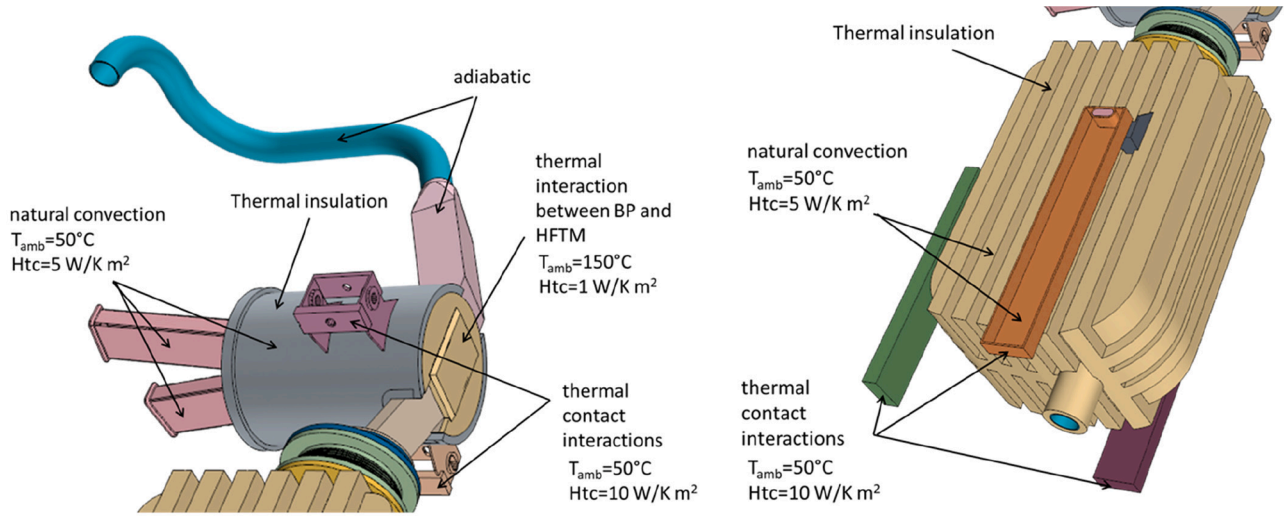

Fig. 9. Heat transfer boundary conditions.

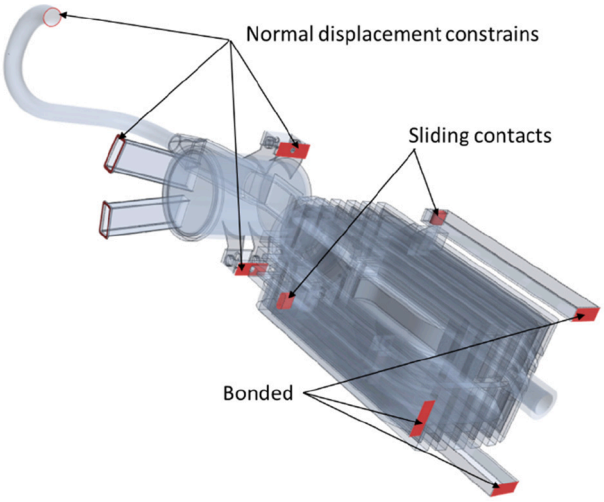

Fig. 10. Mechanical constraints.

The maximum x-displacement of the back plate (BP) in the HFTM direction is approximately 1.3 mm (Fig. 13). It is comparable to the 2 mm gap between BP and HFTM. Although the effect of the thermal expansion of the vacuum chamber is minimized by the bellows, the model does not fully account for the interaction between the beam channel of the vacuum chamber and the beam channels integrated into the test cell wall. This means that an even greater expansion in the direction of HFTM is to be expected. For this reason, the new design of the TA provides a fixed connection between the TA and the HFTM, which ensures a constant distance between the back plate and the outer surface of the HFTM. The maximum thermal expansion of the back plate in the y-direction from the center of the BP is ± 1.4 mm.

Von Mises equivalent stress distribution including primary and secondary stresses is shown.in Fig. 14. From the mechanical point of view an acceptable stress field is generally predicted within the structure of the TA system. High stress values with maximum of 200–250 MPa are calculated in regions with high temperature gradients. The inner side walls in the middle of the target channel are located in the area of the strong nuclear heating. As a result, the wall sections that are not cooled with lithium are heated up to 389 °C. These hotspots cause strong thermal expansion and stresses in the rigid corners.

Summary

This report presents a numerical thermal–hydraulic and structural analysis using updated design of the target system and neutronics analysis results. Simulation scope includes the TA and QT.

Simulations have been conducted with the commercial CFD code Simcenter Star-CCM + . The model combines the CFD and FEM simulations by directly transferring the thermo-hydraulic results into the structural-mechanical model. The other feature of the presented model is the complete mechanical connection between TA and QT. All this can reproduce more realistic behavior of the whole assembly starting from TA inlet pipe to the QT outlet.

The following aspects have been analyzed:

- Temperature distribution in lithium and target system structure during beam-on operation;
- Transient mixing of lithium in the quench tank with temperature change during the beam switch-on phase;
- Thermal displacements and stresses in the TA and QT structures.

Some conclusions can be drawn:

- Simulations using the new distribution of nuclear heating show no significant changes in the temperature field in liquid lithium;
- An acceptable stress field is generally predicted within the structures, although further more detailed structural analysis is needed for final assessments;
- Calculated unwanted temperature hotspots in the target structure demonstrate the need for optimization of the target design;
- The displacement of the BP in the direction of the HFTM is comparable to the fixed gap of 2 mm between two surfaces. This confirms the necessity of the technical solution to keep the distance between the BP and the HFTM constant.

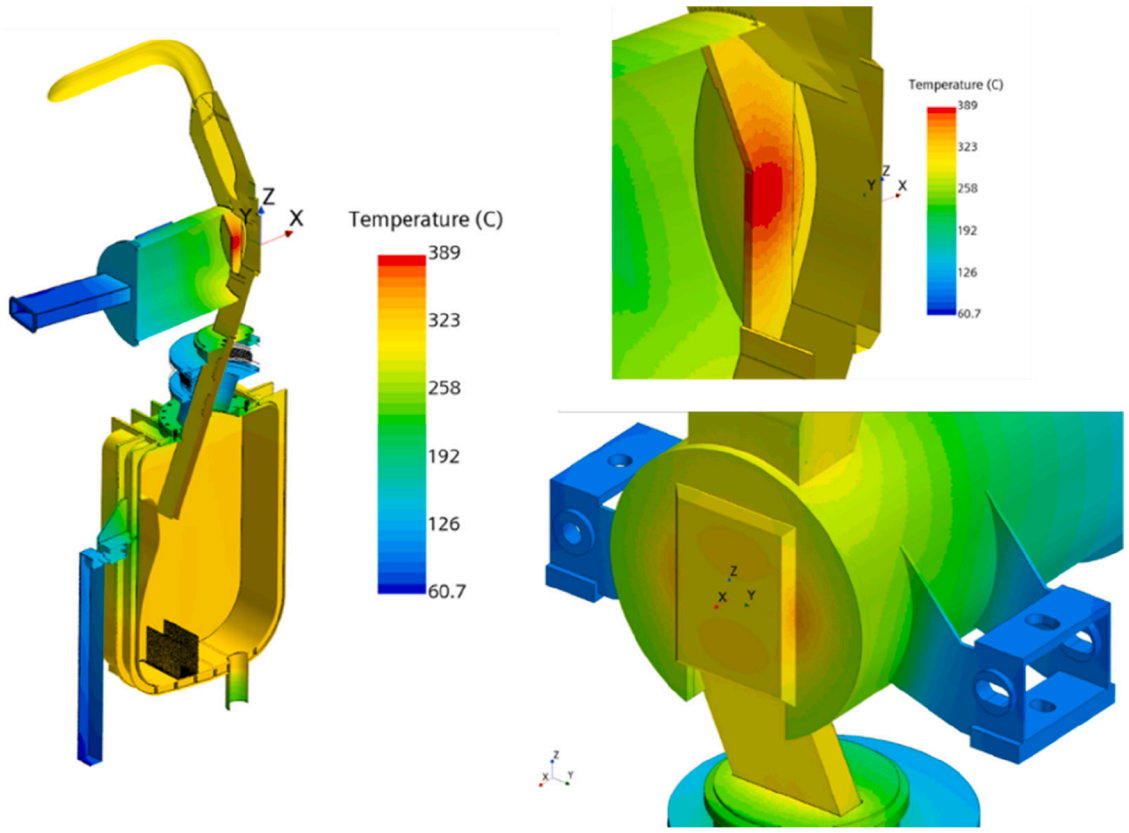

Fig. 11. Temperature field in TA-QT structure.

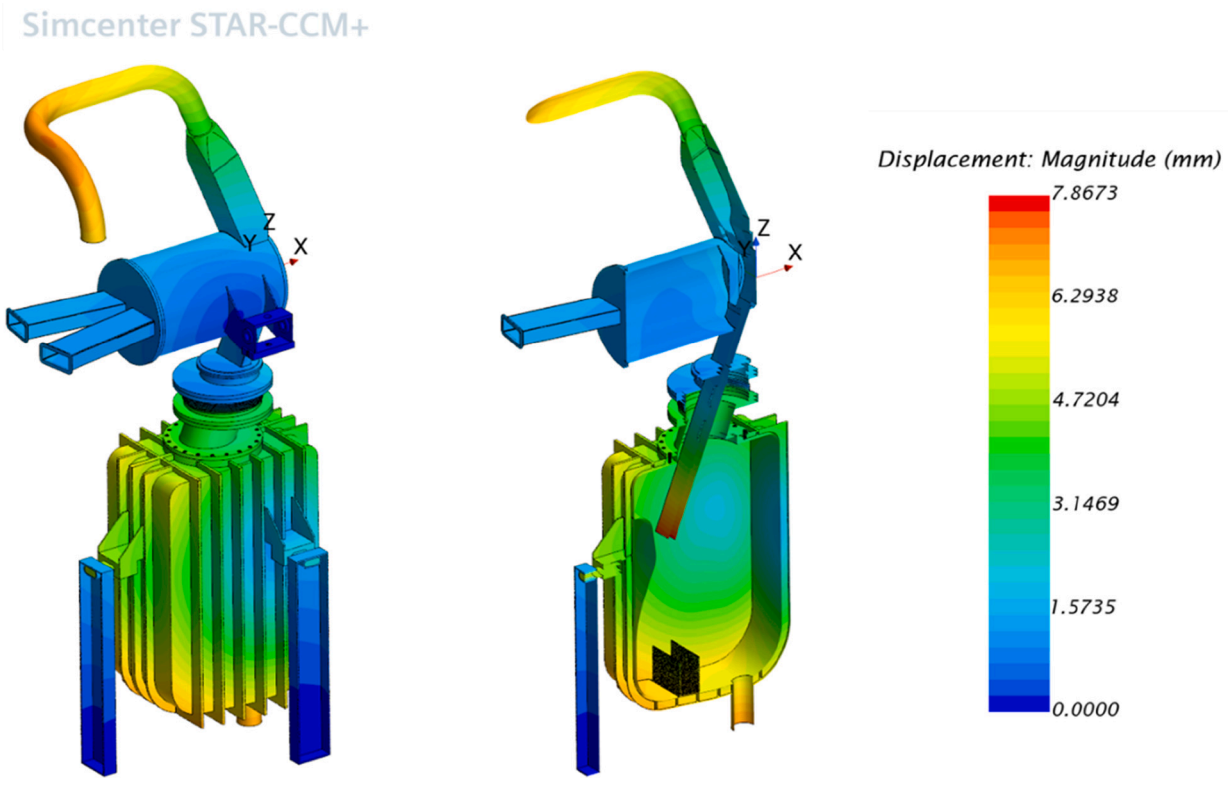

Fig. 12. Thermal displacements.

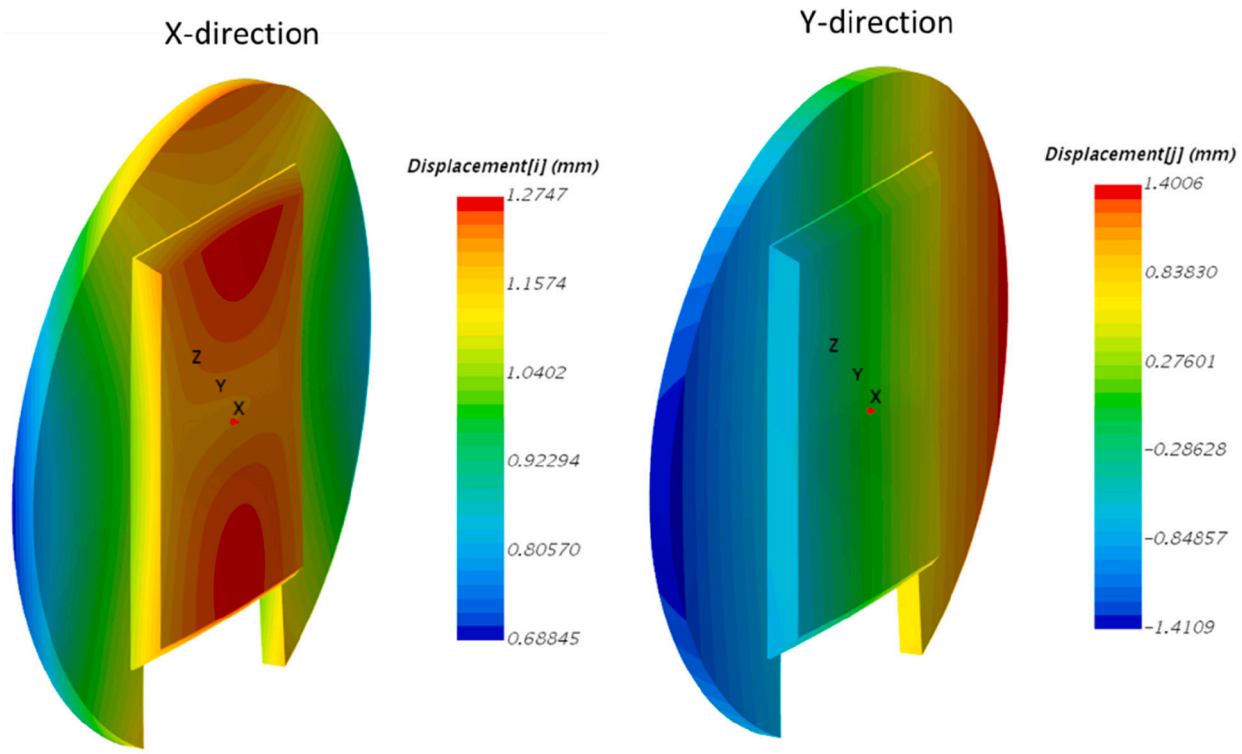

Fig. 13. X and Y displacements of the back plate.

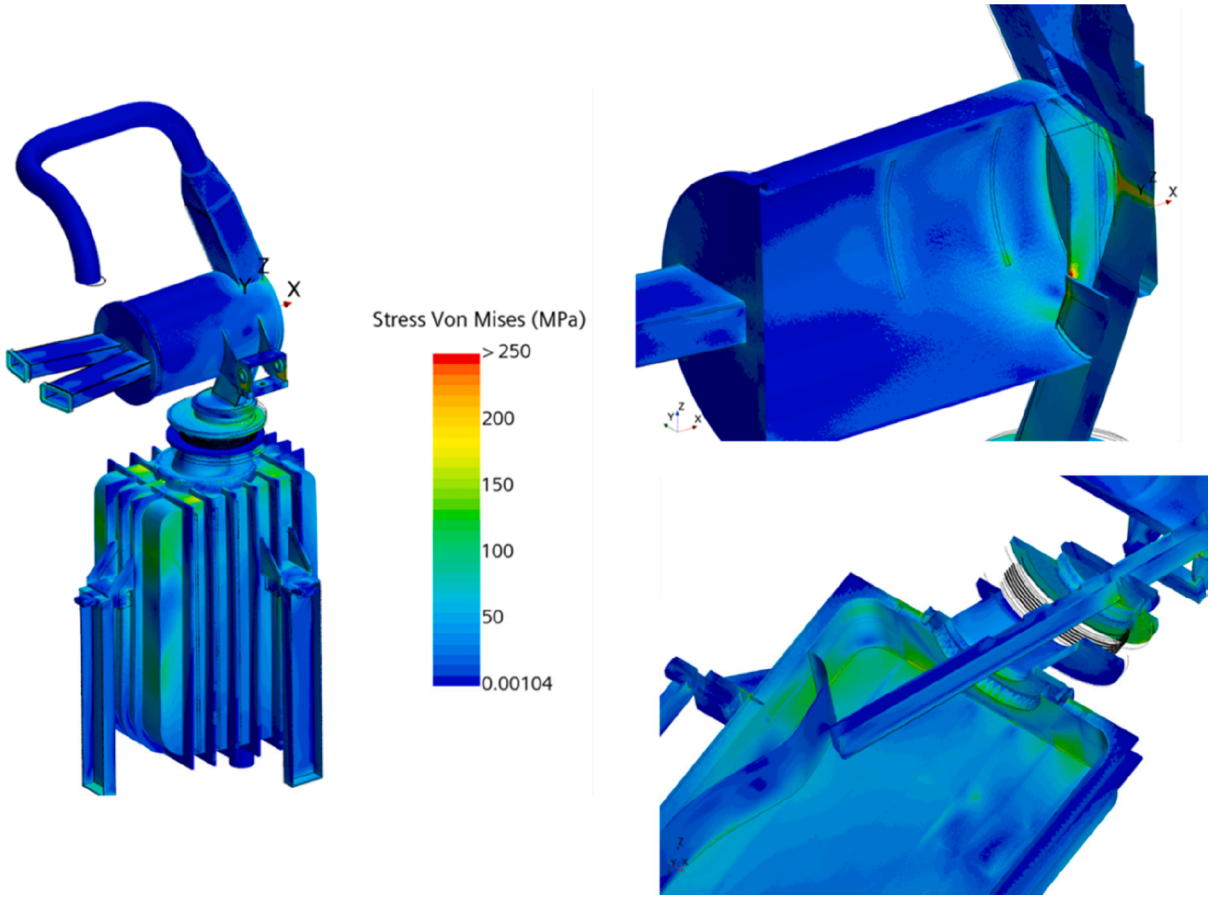

Fig. 14. Von Mises stress distribution in the TA system and in the QT.

CRediT authorship contribution statement

S. Gordeev: Writing – review & editing, Writing – original draft, Visualization, Methodology, Investigation, Conceptualization. **A. Serikov:** Investigation, Data curation. **Y. Qiu:** Investigation, Data curation. **F.S. Nitti:** Project administration, Conceptualization. **J. Maestre:** Project administration, Conceptualization.

Declaration of competing interest

The authors declare that they have no known competing financial interests or personal relationships that could have appeared to influence the work reported in this paper.

Data availability

No data was used for the research described in the article.

Acknowledgments

This work has been carried out within the framework of the EUROfusion Consortium, funded by the European Union via the Euratom Research and Training Programme (Grant Agreement No 101052200 — EUROfusion). Views and opinions expressed are however those of the author(s) only and do not necessarily reflect those of the European Union or the European Commission. Neither the European Union nor the European Commission can be held responsible for them.

References

[1] Ibarra, A, The European approach to the fusion-like neutron source: the IFMIF-DONES project, Nuclear Fusion, Volume 59, Issue 6, article id. 065002 (2019).
[2] D. Tamas et al., Target System (2MQ99Q v1.1), https://idm.euro-fusion.org/?uid=2MQ99Q.
[3] A. Serikov, Y. Qiu, S. Gordeev, Nuclear analyses for the TC with the double layer RBSB concept, Nucl Sci Technol Open Res 1 (2023) 1, https://doi.org/10.21955/nuclscitechnolopenres.1115090.1.
[4] S.P. Simakov, U. Fischer, K. Kondo, P. Pereslavtsev, Status of the Mcdelicious approach for the D-Li neutron source term modeling in IFMIF neutronics calculations, Fusion Sci. Technol. 62 (1) (2012) 233–239, https://doi.org/10.13182/FST11-444.
[5] D. Bernardi, et al., The IFMIF-DONES project: design status and main achievements within the EUROfusion FP8 Work programme, J. Fusion Energ. 41 (2022) 24.
[6] © 2022 Siemens Digital Industries Software.
[7] J. Knaster et al., Overview of the IFMIF/EVEDA project, 2017 Nucl. Fusion 57 102016.
[8] S. Gordeev et al., Analyses of the quench tank configuration for DONES liquid-lithium target system, Fusion Engineering and Design, Volume 136, Part A, November 2018, Pages 330-334.
[9] E. Gaganidze, Material Properties Handbook –EUROFER97 (2020), IDM Ref.: 2NZHBS, https://idm.euro-fusion.org/?uid=2NZHBS.
[10] D. Desai, C. Y. Ho, Thermal linear expansion of nine selected AISI stainless steels. CINDAS report for the American iron and steel institute, April 1978.